Clim. Past Discuss., 8, 621–636, 2012
www.clim-past-discuss.net/8/621/2012/
doi:10.5194/cpd-8-621-2012

Climate of the Past Discussions

Rapid coupling of Antarctic temperature and atmospheric CO_2 during deglaciation

J. B. Pedro[1,2], S. O. Rasmussen[3], and T. D. van Ommen[2,4]

[1]Antarctic Climate & Ecosystems Cooperative Research Centre, University of Tasmania, Hobart, Tasmania, Australia
[2]Institute of Marine and Antarctic Studies, University of Tasmania, Hobart, Tasmania, Australia
[3]Centre for Ice and Climate, University of Copenhagen, Copenhagen, Denmark
[4]Australian Antarctic Division, Kingston, Tasmania, Australia

Received: 31 January 2012 – Accepted: 13 February 2012 – Published: 20 February 2012

Correspondence to: J. B. Pedro (jbpedro@utas.edu.au)

Published by Copernicus Publications on behalf of the European Geosciences Union.

Abstract

Antarctic ice cores provide clear evidence of a close coupling between variations in Antarctic temperature and the atmospheric concentration of CO_2 during the glacial/interglacial cycles of the past 800 thousand years. Precise information on the relative timing of the temperature and CO_2 changes can assist in refining our understanding of the physical processes involved in this coupling. Here, we focus on the last deglaciation, 19 000 to 11 000 years before present, during which CO_2 concentrations increased by ~80 parts per million by volume and Antarctic temperature increased by ~10 °C. Utilising a recently developed proxy for regional Antarctic temperature, derived from five near-coastal ice cores, and two ice core CO_2 records with high dating precision, we show that the increase in CO_2 lagged the increase in regional Antarctic temperature by only 0–400 years. This new value for the lag, consistent for both CO_2 records, implies a faster feedback between temperature and CO_2 than the centennial to millennial-scale lags suggested by previous studies.

1 Introduction

The last deglaciation is the largest naturally-forced global climate change in Earth's recent climate history. Its initial impetus, as with the sequence of glacial/interglacial transitions that came before it, is most commonly attributed to orbitally induced variations in insolation at high northern latitudes (Hays et al., 1976). Amplification through climate feedback processes of the relatively weak orbital signal is then required to explain the full magnitude of the glacial-interglacial climate change (Lorius et al., 1990). Changes in the carbon cycle play a central role among these feedbacks (Lorius et al., 1990; Shackleton, 2000). Mounting evidence attributes a large component of the deglacial CO_2 increase to release of old CO_2 from the deep southern ocean through changes in its biogeochemistry and physical circulation (Anderson et al., 2009; Sigman et al., 2010; Skinner et al., 2010). However, there are open questions about the exact mechanisms involved and their relative contributions (Fischer et al., 2010; Sigman et al., 2010; Toggweiler and Lea, 2010). Determining the timing of the increase in atmospheric CO_2 with respect to the increase in temperature (hereafter "the lag"), is crucial for the models seeking to discriminate between mechanisms (Schmittner and Galbraith, 2008; Ganopolski and Roche, 2009; Lee et al., 2011).

Antarctic ice cores are unique in preserving a record of both temperature variation and atmospheric CO_2 concentration. Water stable isotope ratios ($\delta^{18}O_{ice}$ and δD_{ice}) from the ice are proxies for temperature above the inversion layer at the time of snow formation (Jouzel et al., 1997), while the CO_2 is preserved in air bubbles in the ice. The transformation of snow to glacial ice isolates these bubbles at a depth of 50–100 m, leaving them younger than the surrounding ice by an amount Δ age. The Δ age must therefore be known for the lag between temperature and CO_2 to be accurately determined.

The most commonly cited studies constraining the lag for the last deglaciation have used ice core records from the East Antarctic Plateau (EAP) and report lags of 400–1000 years from Vostok (Fischer et al., 1999) and 200–1400 years from EPICA Dome C (Monnin et al., 2001). Studies of previous deglaciations also suggest millennial-scale lags (Fischer et al., 1999; Mudelsee, 2001; Siegenthaler et al., 2005; Caillon et al., 2003). However, the low accumulation rates at these sites (2–3 $g\,cm^{-2}\,yr^{-1}$) lead to lengthy intervals between deposition and bubble close off, and consequent high values for Δ age: 2400–3300 years for recent times and 4500–5200 years at the last glacial maximum (Fischer et al., 1999; Monnin et al., 2001). These large values are associated with uncertainties of typically 10–20 %, which are comparable to the reported lag values (Loulergue et al., 2007).

The contribution to the lag uncertainty from Δ age can be minimised by considering ice core records from higher accumulation sites. Of the currently available CO_2 records for the deglaciation, those with the lowest Δ ages are the Siple Dome (Ahn et al., 2004) and Byrd (Neftel et al., 1988; Staffelbach et al., 1991) ice cores. The Δ ages at these sites are 200–300 years for recent times and 500–800 years at the last glacial

CPD
8, 621–636, 2012

maximum, an order of magnitude smaller than records from the EAP. Analysis of the Siple Dome stable isotope and CO_2 records suggests lags in the 150–400 year range (Ahn et al., 2004), but this result suffers from the fact that the Siple Dome deglacial isotope record contains abrupt changes not observed in other Antarctic records (Taylor et al., 2004; Brook et al., 2005), suggesting a local climate signal that would not be expected to correlate with CO_2 evolution.

Our approach is to compare the Siple Dome and Byrd CO_2 records to an index of regional Antarctic temperature, T_{proxy}, derived (Pedro et al., 2011) from a composite of high-resolution stable isotope records from the Law Dome, Siple Dome, Byrd, EPICA Dronning Maud Land and Talos Dome ice cores (Fig. 1a, inset shows core locations). Since T_{proxy} contains ice cores representing the Indian, Atlantic, and Pacific coastal Antarctic regions, it is expected to provide a better representation of high-latitude Southern Ocean processes than records from single sites. This approach requires that T_{proxy} and the two CO_2 records share a common timescale. This is achieved by synchronising all records to the Greenland Ice Core Chronology 2005 (GICC05) using the rapid and effectively globally synchronous variations in CH_4 concentrations found in both Antarctic and Greenland ice cores.

2 Materials and methods

2.1 Record synchronisation

The T_{proxy} record is already available on GICC05 (Pedro et al., 2011). We synchronise the timescales of the Siple Dome and Byrd CO_2 records to GICC05 using previously published "gas-age" depth ties from CH_4-based synchronisations of the Byrd (Blunier and Brook, 2001) and Siple Dome (Brook et al., 2005) records with Greenland records. The Byrd CO_2 data on the GRIP SS09 timescale (Johnsen et al., 1997) are transferred via GRIP depth (Blunier and Brook, 2001) to GICC05 ages by linear interpolation using stratigraphical markers (Rasmussen et al., 2008). Similarly, the Siple Dome CO_2

CPD
8, 621–636, 2012

data, on a GISP2 timescale (Ahn et al., 2004) are transferred via GISP2 depth (Meese et al., 1997) to GICC05 ages again by linear interpolation using stratigraphical markers (Rasmussen et al., 2008).

2.2 Lag calculation

We determine lag quantitatively, following previous studies (Fischer et al., 1999; Mudelsee, 2001; Siegenthaler et al., 2005; Ahn et al., 2004), by maximising the time-lagged correlation between the deglacial temperature and CO_2 curves. Two methods are used: first by direct correlation between T_{proxy} and CO_2 (direct method) and second, as used in a prior Siple Dome study (Ahn et al., 2004), by correlation between the corresponding derivative curves, $\partial T_{proxy}/\partial t$ and $\partial CO_2/\partial t$ (derivative method). The derivative method has smaller sensitivity to misidentification of the pre- and post-transition levels at the expense of increased sensitivity to measurement noise, especially in the sections of sparse data. Since it is not clear a priori which approach is superior, we apply both methods in parallel. Prior to the analyses, the CO_2 data are first linearly interpolated to 20-year resolution over the 9–21 ka interval to match the 20-year resolution of T_{proxy}. Derivatives, $\partial T_{proxy}/\partial t$ and $\partial CO_2/\partial t$, are calculated on the same grid. For both methods the data are then smoothed and the time-lagged correlation determined for lags in the −400 to +1000 year range. The robustness of the lag calculation to CO_2 data uncertainty is evaluated by repeating the lag determination 100 times using random realisations of the CO_2 measurements, each sampled using the published uncertainties (represented by the error bars in Fig. 1a).

As the lag shows some sensitivity to the degree of smoothing applied and the overall time interval chosen for assessment we repeated the analysis using 19 different degrees of smoothing and 35 different choices of time interval. The different degrees of smoothing were applied by convolution with a Gaussian filter with a standard deviation ranging from 105–375 years in steps of 15 years; the minimum width of the smoothing corresponds to the approximate sampling rate of CO_2 data in the sparsely sampled parts of the data set, and the maximum was chosen to preserve a clear Antarctic Cold

CPD
8, 621–636, 2012
Rapid coupling of Antarctic temperature and CO_2
J. B. Pedro et al.

Reversal signature. Similar results were obtained by replacing the Gaussian filter with a simple running mean filter of equivalent half-width. The choices of the time interval start and end points for the lag calculation were varied within reasonable limits that encompass the overall deglaciation; specifically, the start and end ages were varied in 200 year steps with the start spanning 19.4–18.2 ka (7 options) and end spanning 12.4–11.6 ka (5 options), as illustrated by the black triangles of Fig. 1a. This covers the start and end of the deglaciation as defined from the perspective of the onset and end of the warming trend in T_{proxy} (Pedro et al., 2011); note that younger than around 11.5 ka both CO_2 curves have high early Holocene values that have no counterpart in the T_{proxy} record. This suggests different processes are responsible and we exclude this period from the correlation interval. The full sensitivity analysis generates 66 500 optimal lag values for each of the direct and derivative methods.

3 Results and discussion

Close correspondence between T_{proxy} and both CO_2 records is observed (Fig. 1a), supporting the hypothesis that marine processes at high southern latitudes are linked to the deglacial CO_2 increase. Visual inspection of the relative timing of the deglacial CO_2 and T_{proxy} increase suggests little or no lag of CO_2 after temperature. Quantitative results on the relative timing are summarised by the four histograms in Fig. 2b. The widths of the individual distributions reflect the sensitivity of the lag values to CO_2 measurement uncertainties, lag determination method (direct or derivative), CO_2 measurement uncertainties, differences between the two CO_2 data sets, smoothing filter widths and the start and end points used in the analysis, as determined by Monte Carlo-style sensitivity analysis. The distributions show larger spread for the derivative method, but overall consistency between the two sites and for the two methods. Using the means and standard deviations quoted in Fig. 2b, we arrive at a weighted value for the lag of 163 years and a methodological uncertainty of 34 years.

CPD
8, 621–636, 2012

We must also consider relative dating uncertainty between T_{proxy} and the two CO_2 records. This uncertainty comprises a component associated with synchronising CH_4 records between multiple cores, σ_{sync}, and a component associated with the Δ age uncertainties of the individual cores, $\sigma_{\Delta age}$. The dating uncertainty in T_{proxy} ,$\sigma_{T_{proxy}}$, ranges from 199–384 years over the time interval considered, with a mean of 269 years (Pedro et al., 2011). The value of σ_{lag} is smaller than $\sigma_{T_{proxy}}$ because σ_{sync} applies to both T_{proxy} and the CO_2 data and thus partially cancels (as seen in the case where data from only one core is used and σ_{sync} cancels completely). The similarity of the results from the independent lag calculation using Siple Dome and Byrd CO_2 data supports that the records are well-synchronised on centennial scales or better. We estimate the contribution to σ_{lag} from $\sigma_{\Delta age}$ and σ_{sync} to be no more than 200 years. This relative dating uncertainty is independent of the abovementioned 34-year methodological uncertainty. Combining the two figures, we arrive at our final estimate that the deglacial CO_2 increase lagged Antarctic temperature by only 0–400 years.

This result is substantially lower and more tightly constrained than the previous Vostok and EPICA Dome C estimates of 200–1400 years and 400–1000 years, albeit consistent within their reported uncertainties. This short lag is supported by more recent empirical constraints indicating that EPICA Dome C Δ age (and thus the CO_2-temperature lag) was significantly overestimated during the last deglaciation (Loulergue et al., 2007). It is important to emphasise that this lag represents an average for the entire deglaciation. Therefore, in a coupled system where multiple processes are likely to be involved in the CO_2 increase (Fischer et al., 2010; Sigman et al., 2010), this value reflects the contributions of all processes weighted by their contribution to the CO_2 increase.

This result shows that the effective combination of these mechanisms operated with little or no lag. Additional observational constraints on the mechanisms are obtained by considering in more detail the millennial and sub-millennial trends in CO_2 throughout the deglaciation. The increase in CO_2, as noted previously (Fischer et al., 1999; Monnin et al., 2001; Ahn et al., 2004), occurs in two main steps. These steps coincide with the two periods of significant warming in T_{proxy} (pink band, Fig. 2) and are separated by a step down in CO_2 concentrations as T_{proxy} exhibits significant cooling within the core of the Antarctic Cold Reversal (dark blue band, Fig. 2). Evidence from Southern Ocean marine sediment cores directly links each of these two warming steps with release of CO_2 accumulated in the deep Southern Ocean during the last glacial period: cores from south of the Antarctic Polar Front show pulses in upwelling (represented by opal fluxes) coinciding with each warming step (Anderson et al., 2009), while cores from the Atlantic sector of the Southern Ocean identify a source of old (^{14}C-depleted) carbon-rich deep water that dissipated over two corresponding intervals (Skinner et al., 2010). An explanation consistent with the reduced lag values identified here, proposes that the increases in upwelling were responsible for the simultaneous delivery of both sequestered heat and CO_2 to the atmosphere around Antarctica (Anderson et al., 2009; Skinner et al., 2010). However, this raises the question of what stimulated the increases in Southern Ocean upwelling.

A clue is provided by examining the time relationship between T_{proxy} and the major millennial and sub-millennial climate events recorded by the North GRIP $\delta^{18}O_{ice}$ record (Fig. 2); i.e. the timing of the well-known bipolar seesaw (Broecker, 1998; Stocker and Johnsen, 2003). Since T_{proxy} and the CO_2 records are synchronised to GICC05, the records from both hemispheres can be directly compared. There is also little or no time lag separating the major millennial and sub millennial climate transitions in Greenland (Lowe et al., 2008) from the onsets and ends of the warming and cooling trends in Antarctica (Pedro et al., 2011). A picture thus emerges from the ice cores of rapid communication between Antarctic temperatures, Greenland temperatures and atmospheric CO_2.

We give attention here to two potentially complimentary mechanisms which appear consistent with these observations. One mechanism supports a greater role for atmospheric pathways (Anderson et al., 2009; Toggweiler and Lea, 2010; Lee et al., 2011) while the other supports a greater role for the ocean (Skinner et al., 2010; Schmittner and Galbraith, 2008). Both mechanisms begin with the discharge of meltwater

CPD
8, 621–636, 2012

and ice into the North Atlantic during Greenland Stadial 2 (Heinrich Stadial 1), possibly due to orbitally driven increases in summer insolation. This causes a collapse of the Atlantic Meridional Overturning Circulation (AMOC) (Ganopolski and Rahmstorf, 2001; McManus et al., 2004). The atmospheric pathway proposes that rapid cooling of the North Atlantic region and sea ice expansion initiates an atmospheric reorganisation in which both the Inter Tropical Convergence Zone and the Southern Hemisphere mid-latitude westerlies are displaced south and/or intensified (Anderson et al., 2009; Toggweiler and Lea, 2010; Lee et al., 2011). The changed westerly regime over the Southern mid- and high-latitude oceans then dissipates sea ice, displaces cold fresh surface waters, drawing up warmer deeper waters which release heat and CO_2. A recent modeling study lends support to this sequence of events and also incorporates an important role for ocean biogeochemical feedbacks (Lee et al., 2011). In line with the constraints identified here, the model supports essentially simultaneous North Atlantic cooling and atmospheric CO_2 release from the high-latitude Southern Ocean, corresponding to an atmospheric CO_2 rise of 20–60 ppm, where the range is dependent on the biological response. However Lee et al. (2011) do not simulate the observed response of Antarctic temperatures, possibly due to fixed Southern Hemisphere sea ice.

The ocean pathway invokes the bipolar seesaw: freshwater-induced collapse of the AMOC reduces northward ocean heat transport, thereby allowing heat to accumulate in the south (Broecker, 1998; Stocker and Johnsen, 2003). This melts back sea ice, removing a physical barrier to the release of CO_2 and exposing the Southern Ocean surface waters to the action of the westerlies. As above, the strengthened westerlies promote upwelling and ventilation of CO_2 from the deep waters (Skinner et al., 2010). The bipolar seesaw, as originally conceived (Broecker, 1998), operates on the millennial timescales of ocean heat transport and hence fails to meet the timing criteria identified here. However, an ocean wave-mediated seesaw (Stocker and Johnsen, 2003) could be capable of sufficiently rapid signal transmission. In one model study, the bipolar-seesaw-induced changes in the circulation modes couple with changes in ocean biogeochemistry and carbon storage in the terrestrial biosphere to produce little or no lag between Greenland and Antarctic temperatures and CO_2 changes (Schmittner and Galbraith, 2008). Unlike, Lee et al. (2011), this model does simulate the observed seesaw-relationship between North Atlantic and Greenland temperatures. Notably, the initial (within the first 250 years) rapid response in CO_2 in Schmittner and Galbraith (2008) is attributed to CO_2 release from the terrestrial biosphere (triggered by cooling associated with the freshwater-induced AMOC collapse) and not to physical or biogeochemical components of the Southern Ocean carbon cycle. However, this does not dismiss the possibility of a rapid ocean CO_2 response to bipolar seesaw-related changes in ocean circulation. Recent studies emphasise the sensitivity of the timescales of ocean ventilation to model resolution; at least under modern boundary conditions, meso-scale eddy-resolving ocean models suggest much faster ventilation times than the coarser resolution models that are currently used for palaeo-simulations (Maltrud et al., 2010).

Current palaeo-modeling efforts appear to be accurately simulating key components of the deglacial sequence of events. However, there is not yet a simulation which fully captures all of the observed trends and phase relationships between Antarctic and North Atlantic temperatures and atmospheric CO_2. The results presented here, with their improved timing constraints over previous studies, provide a more stringent target for future modeling efforts.

4 Conclusions

The ice core observations point to a tightly-coupled system operating with little or no time delay between the onsets/terminations of North-Atlantic climate stages and near-simultaneous trend changes in both Antarctic temperature and atmospheric CO_2. As it stands, the observed timing of events lends support to the current concept of an atmospheric teleconnection between the northern and southern high-latitudes, which forces wind-driven CO_2 release from the Southern Ocean. However, sorting out the relative roles of atmospheric and oceanic coupling mechanisms and the interactions between them remains a major challenge. More densely sampled and higher precision CO_2 measurements from high-accumulation ice core sites may assist with constraining the time evolution of the temperature/CO_2 lag during different stages of the deglaciation. However, if the response in the Southern Hemisphere is instantaneous, then higher resolution records may not be sufficient. Further progress in understanding these mechanisms requires more work at the interface between palaeoclimate observation and Earth system modeling, in particular modeling efforts to more tightly constrain the potential timescales of bipolar seesaw-induced changes in CO_2 ventilation.

The T_{proxy} series is archived at the Australian Antarctic Data Center (http://data.aad.gov.au/) and at the World Data Center for Paleoclimatology (http://www.ncdc.noaa.gov/paleo/). The CO_2 records on the GICC05 timescale will be similarly archived following publication.

Acknowledgements. This work was assisted by the Australian Government's Cooperative Research Centres Programme, through the Antarctic Climate and Ecosystems Cooperative Research Centre (ACE CRC). Travel support from an Inge Lehmann grant (SOR), the Trans-Antarctic Association and INQUA/INTIMATE (JBP) made this collaboration possible.

References

Ahn, J., Wahlen, M., Deck, B. L., Brook, E. J., Mayewski, P. A., Taylor, K. C., and White, J. W. C.: A record of atmospheric CO_2 during the last 40,000 years from the Siple Dome, Antarctica ice core, J. Geophys. Res., 109, D13305, doi:10.1029/2003JD004415, 2004. 623, 624, 625, 627

Anderson, R. F., Ali, S., Bradtmiller, L. I., Nielsen, S. H. H., Fleisher, M. Q., Anderson, B. E., and Burckle, L. H.: Wind-driven upwelling in the Southern Ocean and the deglacial rise in atmospheric CO_2, Science, 323, 1443–1448, doi:10.1126/science.1167441, 2009. 622, 628, 629

Blunier, T. and Brook, E. J.: Timing of millennial-scale climate change in Antarctica and Greenland during the last glacial period, Science, 291, 109–112, doi:10.1126/science.291.5501.109, 2001. 624

Broecker, W.: Palaeocean circulation during the last deglaciation: A bipolar seesaw?, Paleoceanography, 13, 119–121, doi:10.1029/97PA03707, 1998. 628, 629

Brook, E. J., White, J. W. C., Schilla, A. S. M., Bender, M. L., Barnett, B., Severinghaus, J. P., Taylor, K. C., Alley, R. B., and Steig, E. J.: Timing of millennial-scale climate change at Siple Dome, West Antarctica, during the last glacial period, Quaternary Sci. Rev., 24, 1333–1343, doi:10.1016/j.quascirev.2005.02.002, 2005. 624

Caillon, N., Severinghaus, J. P., Jouzel, J., Barnola, J.-M., Kang, J., and Lipenkov, V. Y.: Timing of atmospheric CO_2 and Antarctic temperature changes across termination III, Science, 299, 1728–1731, doi:10.1126/science.1078758, 2003. 623

Fischer, H., Wahlen, M., Smith, J., Mastroianni, D., and Deck, B.: Ice core records of atmospheric CO_2 around the last three glacial terminations, Science, 283, 1712–1714, doi:10.1126/science.283.5408.1712, 1999. 623, 625, 627

Fischer, H., Schmitt, J., Lüthi, D., Stocker, T. F., Tschumi, T., Parekh, P., Joos, F., Köhler, P., Völker, C., Gersonde, R., Barbante, C., Le Floch, M., Raynaud, D., and Wolff, E.: The role of Southern Ocean processes in orbital and millennial CO_2 variations – A synthesis, Quaternary Sci. Rev., 29, 193–205, doi:10.1016/j.quascirev.2009.06.007, 2010. 623, 627

Ganopolski, A. and Rahmstorf, S.: Rapid changes of glacial climate simulated in a coupled climate model, Nature, 409, 153–158, 2001. 629

Ganopolski, A. and Roche, D. M.: On the nature of lead-lag relationships during glacial-interglacial climate transitions, Quaternary Sci. Rev., 28, 3361–3378, 2009. 623

Hays, J. D., Imbrie, J., and Shackleton, N. J.: Variations in the Earth's orbit: Pacemaker of the ice ages, Science, 194, 1121–1132, doi:10.1126/science.194.4270.1121, 1976. 622

Johnsen, S. J., Clausen, H. B., Dansgaard, W., Gundestrup, N. S., Hammer, C. U., Andersen, U., Andersen, K. K., Hvidberg, C. S., Dahl-Jensen, D., Steffensen, J. P., Shoji, H., Sveinbjörnsdóttir, Á. E., White, J., Jouzel, J., and Fisher, D.: The $\delta^{18}O$ record along the Greenland Ice Core Project deep ice core and the problem of possible Eemian climatic instability, J. Geophys. Res., 102, 26397–26410, doi:10.1029/97JC00167, 1997. 624

Jouzel, J., Alley, R. B., Cuffey, K. M., Dansgaard, W., Grootes, P., Hoffmann, G., Johnsen, S. J., Koster, R. D., Peel, D., Shuman, C. A., Stievenard, M., Stuiver, M., and White, J.: Validity of the temperature reconstruction from water isotopes in ice cores, J. Geophys. Res., 1022,

26471–26488, doi:10.1029/97JC01283, 1997. 623
Lee, S.-Y., Chiang, J. C. H., Matsumoto, K., and Tokos, K. S.: Southern Ocean wind response to North Atlantic cooling and the rise in atmospheric CO_2: Modeling perspective and paleoceanographic implications, Paleoceanography, 26, PA1214, doi:10.1029/2010PA002004, 2011. 623, 628, 629, 630
Lorius, C., Raynaud, D., Jouzel, J., Hansen, J., and Le Treut, H.: The ice-core record – Climate sensitivity and future greenhouse warming, Nature, 347, 139–145, doi:10.1038/347139a0, 1990. 622
Loulergue, L., Parrenin, F., Blunier, T., Barnola, J.-M., Spahni, R., Schilt, A., Raisbeck, G., and Chappellaz, J.: New constraints on the gas age-ice age difference along the EPICA ice cores, 0–50 kyr, Clim. Past, 3, 527–540, doi:10.5194/cp-3-527-2007, 2007. 623, 627
Lowe, J. J., Rasmussen, S. O., Björck, S., Hoek, W. Z., Steffensen, J. P., Walker, M. J. C., and Yu, Z. C.: Synchronisation of palaeoenvironmental events in the North Atlantic region during the Last Termination: a revised protocol recommended by the INTIMATE group, Quaternary Sci. Rev., 27, 6–17, doi:10.1016/j.quascirev.2007.09.016, 2008. 628, 636
Maltrud, M., Bryan, F., and Peacock, S.: Boundary impulse response functions in a century-long eddying global ocean simulation, Environ. Fluid Mech., 10, 275–295, 2010. 630
McManus, J. F., Francois, R., Gherardi, J.-M., Keigwin, L. D., and Brown-Leger, S.: Collapse and rapid resumption of Atlantic meridional circulation linked to deglacial climate changes, Nature, 428, 834–837, doi:10.1038/nature02494, 2004. 629
Meese, D. A., Gow, A. J., Alley, R. B., Zielinski, G. A., Grootes, P. M., Ram, M., Taylor, K. C., Mayewski, P. A., and Bolzan, J. F.: The Greenland Ice Sheet Project 2 depth-age scale: Methods and results, J. Geophys. Res., 102, 26411–26424, doi:10.1029/97JC00269, 1997. 625
Monnin, E., Indermühle, A., Dällenbach, A., Flückiger, J., Stauffer, B., Stocker, T. F., Raynaud, D., and Barnola, J.-M.: Atmospheric CO_2 concentrations over the last glacial termination, Science, 291, 112–114, doi:10.1126/science.291.5501.112, 2001. 623, 627
Mudelsee, M.: The phase relations among atmospheric CO2 content, temperature and global ice volume over the past 420 ka, Quaternary Sci. Rev., 20, 583–589, doi:10.1016/S0277-3791(00)00167-0, 2001. 623, 625
Neftel, A., Oeschger, H., Staffelbach, T., and Stauffer, B.: CO_2 record in the Byrd ice core 50,000–5,000 years bp, Nature, 331, 609–611, doi:10.1038/331609a0, 1988. 623

CPD
8, 621–636, 2012

Rapid coupling of Antarctic temperature and CO_2

J. B. Pedro et al.

Pedro, J. B., van Ommen, T. D., Rasmussen, S. O., Morgan, V. I., Chappellaz, J., Moy, A. D., Masson-Delmotte, V., and Delmotte, M.: The last deglaciation: timing the bipolar seesaw, Clim. Past, 7, 671–683, doi:10.5194/cp-7-671-2011, 2011. 624, 626, 627, 628, 636

Rasmussen, S. O., Seierstad, I. K., Andersen, K. K., Bigler, M., Dahl-Jensen, D., and Johnsen, S. J.: Synchronization of the NGRIP, GRIP, and GISP2 ice cores across MIS 2 and palaeoclimatic implications, Quaternary Sci. Rev., 27, 18–28, doi:10.1016/j.quascirev.2007.01.016, 2008. 624, 625

Schmittner, A. and Galbraith, E. D.: Glacial greenhouse-gas fluctuations controlled by ocean circulation changes, Nature, 456, 373–376, doi:10.1038/nature07531, 2008. 623, 628, 630

Shackleton, N. J.: The 100,000-year ice-age cycle identified and found to lag temperature, carbon dioxide, and orbital eccentricity, Science, 289, 1897–1902, doi:10.1126/science.289.5486.1897, 2000. 622

Siegenthaler, U., Stocker, T. F., Monnin, E., Lüthi, D., Schwander, J., Stauffer, B., Raynaud, D., Barnola, J.-M., Fischer, H., Masson-Delmotte, V., and Jouzel, J.: Stable carbon cycle-climate relationship during the late Pleistocene, Science, 310, 1313–1317, doi:10.1126/science.1120130, 2005. 623, 625

Sigman, D. M., Hain, M. P., and Haug, G. H.: The polar ocean and glacial cycles in atmospheric CO_2 concentration, Nature, 466, 47–55, 2010. 622, 623, 627

Skinner, L. C., Fallon, S., Waelbroeck, C., Michel, E., and Barker, S.: Ventilation of the deep Southern Ocean and deglacial CO_2 rise, Science, 328, 1147–1151, doi:10.1126/science.1183627, 2010. 622, 628, 629

Staffelbach, T., Stauffer, B., Sigg, A., and Oeschger, H.: CO_2 measurements from polar ice cores – More data from different sites, Tellus B, 43, 91–96, doi:10.1034/j.1600-0889.1991.t01-1-00003.x, 1991. 623

Stocker, T. F. and Johnsen, S. J.: A minimum thermodynamic model for the bipolar seesaw, Paleoceanography, 18, 1087, doi:10.1029/2003PA000920, 2003. 628, 629

Taylor, K. C., White, J. W. C., Severinghaus, J. P., Brook, E. J., Mayewski, P. A., Alley, R. B., Steig, E. J., Spencer, M. K., Meyerson, E., Meese, D. A., Lamorey, G. W., Grachev, A., Gow, A. J., and Barnett, B. A.: Abrupt climate change around 22 ka on the Siple Coast of Antarctica, Quaternary Sci. Rev., 23, 7–15, doi:10.1016/j.quascirev.2003.09.004, 2004. 624

Toggweiler, J. R. and Lea, D. W.: Temperature differences between the hemispheres and ice age climate variability, Paleoceanography, 25, PA2212, doi:10.1029/2009PA001758, 2010. 623, 628, 629

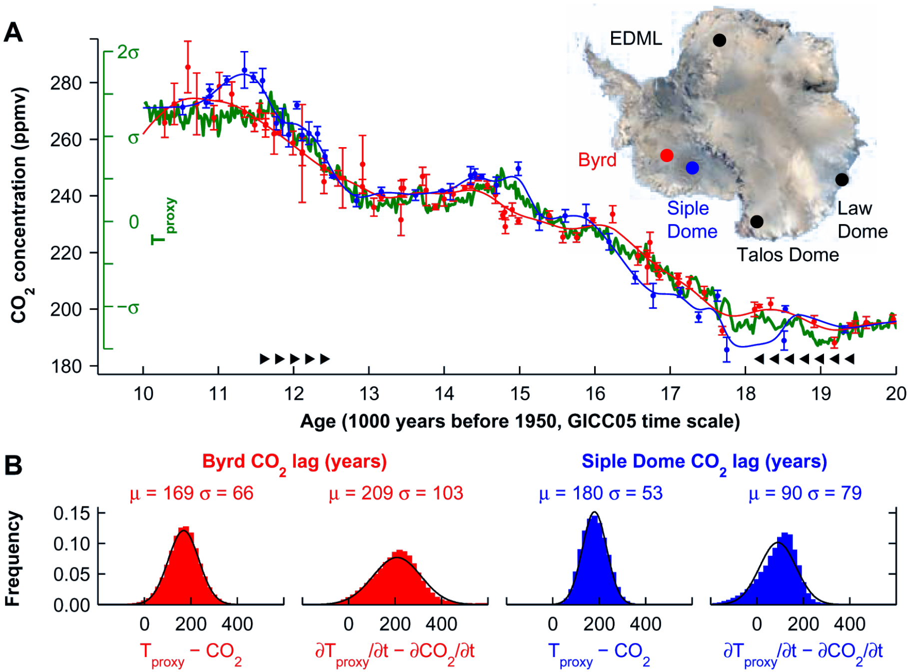

Fig. 1. The phase relationship between regional Antarctic temperature and atmospheric CO_2. **A)** Antarctic temperature proxy T_{proxy} (green) and CO_2 data (1 σ error bars) from Byrd (red) and Siple Dome (blue) on the GICC05 timescale. In the example shown, the CO_2 curves have been smoothed with a Gaussian filter of width 105 years. **(B)** Lag histograms for the two lag determination techniques, direct correlation and correlation of derivatives, using each of the two CO_2 data sets (red, blue) and the best fit of Gaussian distributions (black curves and μ and σ values). The histogram widths reflect each lag determination's sensitivity to the degree of data smoothing, CO_2 measurement uncertainties and different choices of lag calculation data interval start and end points – black triangles in part **(A)**. The map shows the location of the Antarctic ice core sites from which data have been used (source: NASA).

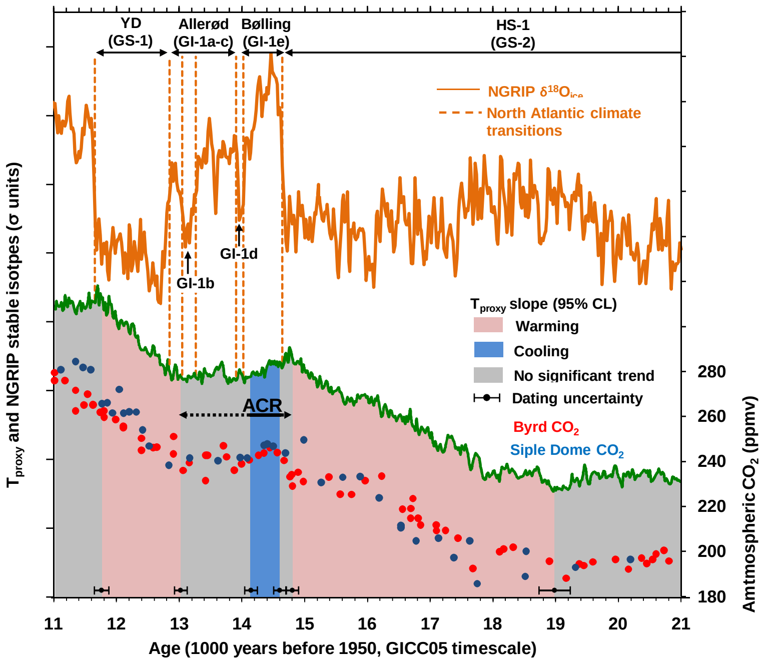

Fig. 2. Atmospheric CO_2 and the bipolar seesaw on the GICC05 timescale. Significant warming and cooling trends in T_{proxy} are represented by coloured vertical bands, adopted from a previous study (Pedro et al., 2011). Climate in the North Atlantic region is represented by the NorthGRIP ice core $\delta^{18}O$ record (Lowe et al., 2008). Changes in the slope of T_{proxy} are synchronous with climate transitions in the North Atlantic (vertical orange lines) within relative dating uncertainties (horizontal error bars). The deglacial increase in CO_2 occurs in two steps, corresponding to the significant warming trends in T_{proxy} (pink bands). A pause in the CO_2 rise is aligned with a break in the warming trend (central grey band) during the Antarctic Cold Reversal (ACR). Within the core of the Antarctic Cold Reversal significant cooling in T_{proxy} (dark blue band), coincides with an apparent decrease in CO_2. Fast-acting inter-hemispheric coupling mechanisms linking Antarctica, Greenland and the Southern Ocean are required to satisfy these timing constraints.

CPD
8, 621–636, 2012

Rapid coupling of Antarctic temperature and CO_2

J. B. Pedro et al.